Direct numerical simulations of turbulent non-premixed methane-air flames modeled with reduced kinetics

By J. M. Card[1], J. H. Chen[1], M. Day[2], AND S. Mahalingam[3]

Turbulent non-premixed stoichiometric methane-air flames modeled with reduced kinetics have been studied using the direct numerical simulation approach. The simulations include realistic chemical kinetics, and the molecular transport is modeled with constant Lewis numbers for individual species. The effect of turbulence on the internal flame structure and extinction characteristics of methane-air flames is evaluated. Consistent with earlier DNS with simple one-step chemistry, the flame is wrinkled and in some regions extinguished by the turbulence, while the turbulence is weakened in the vicinity of the flame due to a combination of dilatation and an increase in kinematic viscosity. Unlike previous results, reignition is observed in the present simulations. Lewis number effects are important in determining the local stoichiometry of the flame. The results presented in this work are preliminary but demonstrate the feasibility of incorporating reduced kinetics for the oxidation of methane with direct numerical simulations of homogeneous turbulence to evaluate the limitations of various levels of reduction in the kinetics and to address the formation of thermal and prompt NO_x.

1. Introduction

During the 1992 CTR summer program we studied the influence of finite-rate chemistry and transient effects on the structure of a turbulent non-premixed flame using DNS (Chen et al. 1992a, 1992b, Mahalingam et al. 1994). In this DNS, the combustion chemistry was approximated by an Arrhenius single- and two-step model. While these simple mechanisms provide useful insights for modeling under conditions ranging from near equilibrium to near extinction, they do not, however, relate the flame structure and extinction characteristics to the underlying elementary chemical-kinetic steps (typically more than 100 reactions) necessary to describe the combustion process in hydrocarbons. But the incorporation of such detailed chemistry for simulations at turbulent Reynolds numbers of practical interest is technologically infeasible at the present time. Thus, it is desirable to introduce reduced chemical-kinetic mechanisms for the description of the combustion chemistry (Smooke 1991). These mechanisms are deduced from a detailed mechanism by

1 Sandia National Laboratories
2 Stanford University
3 University of Colorado at Boulder

the systematic application of steady-state approximations for intermediate species. The combustion kinetics are then described by a few (two to five) global reactions, in which only the most elementary kinetic steps are retained and the concentrations of various intermediate species are represented by algebraic relations.

Computations employing reduced mechanisms have successfully been accomplished for laminar, planar hydrocarbon, and hydrogen flames (Peters and Rogg 1993). Recent progress has also been made using reduced kinetics in simulations of reacting flows of $H_2 - O_2$ systems (Baum *et al.* 1992, and Montgomery *et al.* 1993).

The primary objective of this study is to evaluate the effect of different levels of reduction of fuel oxidation kinetics on methane-air turbulent diffusion flame structure and extinction characteristics.

2. Reduced chemistry for flame structure

The oxidation of methane can be described by the following reduced mechanism (Seshadri and Peters 1988):

$$\mathrm{CH_4 + 2H + H_2O \rightleftharpoons CO + 4H_2}, \qquad \mathrm{I'}$$

$$\mathrm{CO + H_2O \rightleftharpoons CO_2 + H_2}, \qquad \mathrm{II'}$$

$$\mathrm{2H + M \rightleftharpoons H_2 + M}, \qquad \mathrm{III'}$$

$$\mathrm{O_2 + 3H_2 \rightleftharpoons 2H + 2H_2O}. \qquad \mathrm{IV'}$$

These global reactions were deduced from a 40-some-step starting mechanism by the systematic application of steady-state assumptions for the intermediate species. The global rates for the above reaction can be expressed in terms of the elementary rates shown in Table 1, namely

$$\omega_{\mathrm{I'}} = \omega_{\mathrm{I}} = k_{38f}[\mathrm{CH_4}][\mathrm{H}], \tag{1}$$

$$\omega_{\mathrm{II'}} = \omega_{\mathrm{II}} = (k_{18f}/K_3)[\mathrm{H}]([\mathrm{CO}][\mathrm{H_2O}]/[\mathrm{H_2}] - [\mathrm{CO_2}]/(K_{18}/K_3)), \tag{2}$$

$$\omega_{\mathrm{III'}} = \omega_{\mathrm{III}} = k_{5f}[\mathrm{H}][\mathrm{O_2}][M], \tag{3}$$

$$\omega_{\mathrm{IV}} = k_{1f}[\mathrm{H}]([\mathrm{O_2}] - [\mathrm{H}]^2[\mathrm{H_2O}]^2/[\mathrm{H_2}]^3 K_1 K_2 K_3^2), \tag{4}$$

where partial equilibria were assumed for elementary steps (2) and (3). In the above rates, the K's are equilibrium constants, the k's are the elementary rate constants, in which the numbering is selected to agree with Peters and Rogg (1993), and where i is the concentration of species i. Moreover, the concentration of the third body is $[M] = 6.5[\mathrm{CH_4}] + 6.5[\mathrm{H_2O}] + 1.5[\mathrm{CO_2}] + 0.75[\mathrm{CO}] + 0.4[\mathrm{O_2}] + 0.4[\mathrm{N_2}] + 1.0[\mathrm{other}]$.

If we further assume that the H atom is in steady state, we get

$$\omega_{\mathrm{IV'}} = \omega_{\mathrm{I'}} + \omega_{\mathrm{III'}},$$

and the four-step mechanism reduces to the three-step approximation

$$\mathrm{CH_4 + O_2 \rightleftharpoons CO + H_2 + H_2O}, \qquad \mathrm{I}$$

$$CO + H_2O \rightleftharpoons CO_2 + H_2, \qquad \text{II}$$

$$O_2 + 2H_2 \rightleftharpoons 2H_2O, \qquad \text{III}$$

with rates for steps I, II, and II given by Eqs. (1-3), respectively.

Equations (1),(3), and (4) may be employed to show that

$$[H] = (1 - k_{38f}[CH_4]/(k_{1f}[O_2]) - k_{5f}[M]/k_{1f})^{1/2}[O_2]^{1/2}[H_2]^{3/2}(K_1K_2)^{1/2}K_3/[H_2O].$$

Assuming partial equilibrium for the water-gas shift (eq. II) results in a two-step mechanism, and a one-step mechanism may be obtained by assuming H_2 (and hence, CO also) to be in steady state. The rate for the global step $CH_4 + 2O_2 \rightarrow CO_2 + 2H_2O$ is taken from Bui-Pham (1992), namely, $k = 5.2 \times 10^{13}\exp(-14906/T)$ (units are moles, cm, s , degK, and KJ/mole). For comparative purposes, future calculations will consider the rate constant determined by Puri (1987).

The four-, three-, and 1-step kinetic mechanisms and the corresponding global rates are the basis for the present study.

3. Governing equations and numerical method

The governing equations are the continuity, momentum, species, and energy equations written in Cartesian tensor notation as follows:

$$\frac{\partial \rho}{\partial t} + \frac{\partial \rho u_j}{\partial x_j} = 0\,, \tag{5}$$

$$\frac{\partial \rho u_i}{\partial t} + \frac{\partial \rho u_i u_j}{\partial x_j} = -\frac{\partial p}{\partial x_i} + \frac{\partial \tau_{ij}}{\partial x_j}\,, \tag{6}$$

$$\frac{\partial \rho Y_\alpha}{\partial t} + \frac{\partial \rho Y_\alpha u_j}{\partial x_j} = -\frac{\partial}{\partial x_j}(\rho Y_\alpha V_{\alpha j}) + \dot{\omega_\alpha} \tag{7}$$

$$\frac{\partial \rho e_t}{\partial t} + \frac{\partial (\rho e_t + p)u_j}{\partial x_j} = \frac{\partial (u_i \tau_{ij})}{\partial x_j} - \frac{\partial q_j}{\partial x_j} \tag{8}$$

where

$$\tau_{ij} = \mu\Big(\frac{\partial u_i}{\partial x_j} + \frac{\partial u_j}{\partial x_i} - \frac{2}{3}\delta_{ij}\frac{\partial u_k}{\partial x_k}\Big)\,, \tag{9}$$

is the stress tensor,

$$e_t = e + \frac{1}{2}\sum_{k=1}^{3} u_k^2, \quad e = \sum_{\alpha=1}^{N} Y_\alpha h_\alpha - \frac{p}{\rho} \tag{10}$$

is the total energy per unit mass of the mixture, e is the internal energy per unit mass, h_α is the enthalpy of species α given by,

$$h_\alpha = h_\alpha^0 + \int_{T^0}^{T} C_{p\alpha}(T')dT', \quad \alpha = 1, \cdots, N \tag{11}$$

where h_α^0 and $C_{p\alpha}$ are the corresponding enthalpy of formation and specific heat at constant pressure respectively. The heat flux vector is given by

$$q_j = -\lambda \frac{\partial T}{\partial x_j} + \rho \sum_{\alpha=1}^{N} h_\alpha Y_\alpha V_{\alpha j} \tag{12}$$

and the species diffusion velocity is

$$V_{\alpha j} = -D_{\alpha N} \frac{1}{Y_\alpha} \frac{\partial Y_\alpha}{\partial x_j}, \quad \alpha = 1, \cdots N-1 \tag{13}$$

where $D_{\alpha N}$ is the binary diffusion coefficient between species α and the N-th species taken to be nitrogen. To ensure that the net diffusion velocity is zero, the constraint $\sum_{\alpha=1}^{N} Y_\alpha V_{\alpha j} = 0$ is enforced to obtain V_{Nj}. The equation of state is

$$p = \rho R T \tag{14}$$

where R is the mixture gas constant given by

$$R = R^0/\bar{W}, \quad \bar{W} = \left[\sum_{\alpha=1}^{N} \left(\frac{Y_\alpha}{W_\alpha} \right) \right]^{-1} \tag{15}$$

where R^0 is the universal gas constant, $\bar{W}$ is the average molecular weight of the mixture, and W_α is the species molecular weight. The mixture averaged thermal conductivity is modeled through the approximation suggested by Smooke and Giovangigli (1991),

$$\lambda = \bar{C}_p A \left(\frac{T}{T_0} \right)^r \qquad \bar{C}_p(T) = \sum_{\alpha=1}^{N} Y_\alpha C_{p\alpha}(T) \tag{16}$$

where $A = 2.58 \times 10^{-4}$ g/cm-sec, $r = 0.7$, and $\bar{C}_p$ is the specific heat of the gaseous mixture. The individual species specific heats are obtained as polynomial functions of temperature using the Chemkin thermodynamic database (Kee *et al.* 1987). The diffusion coefficients are obtained by prescription of Lewis numbers for individual species through

$$D_{\alpha N} = \frac{\lambda}{\bar{C}_p \rho L e_\alpha}. \tag{17}$$

The Lewis number data is obtained from Smooke and Giovangigli (1991). For the one-step mechanism, the Lewis numbers for CH_4, O_2, CO_2, and H_2O are 0.97, 1.11, 1.39, and 0.83, respectively, for the three-step mechanism, the additional Lewis numbers for H_2 and CO (0.3 and 1.1, respectively) were employed, and for the four-step mechanism, the Lewis number for H is 0.18. The other symbols in these equations have the usual meaning.

For the three-step reduced mechanism, conservation equations for six reacting species is considered (CH_4, O_2, CO_2, CO, H_2, and H_2O) and the mass fraction of

N_2 is obtained through the relationship $\sum_{\alpha=1}^{N} Y_\alpha = 1$, where $N = 7$. Based on the discussion in the previous section, the reaction rates for the six species is computed through the following expressions:

$$\dot{\omega}_{CH_4} = -W_{CH_4}\dot{\omega}_I, \quad \dot{\omega}_{O_2} = -W_{O_2}[\dot{\omega}_I + \dot{\omega}_{III}], \quad \dot{\omega}_{CO_2} = W_{CO_2}\dot{\omega}_{II},$$

$$\dot{\omega}_{CO} = W_{CO}[\dot{\omega}_I - \dot{\omega}_{II}], \quad \dot{\omega}_{H_2} = W_{H_2}[\dot{\omega}_I + \dot{\omega}_{II} - 2\dot{\omega}_{III}], \tag{18}$$

and,

$$\dot{\omega}_{H_2O} = W_{H_2O}[\dot{\omega}_I - \dot{\omega}_{II} + 2\dot{\omega}_{III}].$$

For the four-step mechanism, $N = 8$, and seven reacting species (CH_4, O_2, CO_2, CO, H_2, H_2O, and H) are considered. The reaction rate for these species is given by:

$$\dot{\omega}_{CH_4} = -W_{CH_4}\dot{\omega}_I, \quad \dot{\omega}_{O_2} = -W_{O_2}\dot{\omega}_{IV}, \quad \dot{\omega}_{CO_2} = W_{CO_2}\dot{\omega}_{II},$$

$$\dot{\omega}_{CO} = W_{CO}[\dot{\omega}_I - \dot{\omega}_{II}], \quad \dot{\omega}_{H_2} = W_{H_2}[4\dot{\omega}_I + \dot{\omega}_{II} + \dot{\omega}_{III} - 3\dot{\omega}_{IV}], \tag{19}$$

and,

$$\dot{\omega}_{H_2O} = W_{H_2O}[2\dot{\omega}_{IV} - \dot{\omega}_{II} - \dot{\omega}_I], \quad \dot{\omega}_H = 2\dot{\omega}_{IV} - 2\dot{\omega}_I - 2\dot{\omega}_{III}.$$

The dimensionless form of the governing equations is obtained through definition of appropriate reference quantities based on the air stream properties. The sound speed at infinity a_∞, corresponding density ρ_∞, and the dynamic pressure $\rho_\infty a_\infty^2$ are used for the velocity, density, and pressure reference quantities. The reference temperature is $(\gamma_\infty - 1)T_\infty$ where γ_∞ is the ratio of specific heats at temperature T_∞ of the air stream. The reference fluid properties used are μ_∞, λ_∞, and $C_{p\infty}$ corresponding to air at temperature T_∞. A reference length scale L_{ref} is chosen to be the distance between the fuel and oxidizer jets in the opposed diffusion flame used to initialize all the dependent variables in the computational domain. The equations are solved using a standard sixth-order accurate compact finite differencing scheme (Lele, 1992) for approximating spatial derivatives, and a third-order Runge-Kutta scheme for time advancement. A modified version of the Navier-Stokes Characteristic Boundary Condition (NSCBC) procedure originally developed by Poinsot and Lele (1992), and suitably modified to account for variable specific heats is implemented. The boundary conditions are periodic in the y direction and non-reflecting in the x direction (see Chen *et al.*, 1992a).

The turbulence field is prescribed by an initial two-dimensional turbulent kinetic energy spectrum function

$$E(k) = C_0 \frac{u_0^2}{k_0} \left(\frac{k}{k_0}\right)^4 \exp\left[-2\left(\frac{k}{k_0}\right)^2\right], \tag{20}$$

where k is the wavenumber, k_0 is the wavenumber corresponding to the most energetic eddies, and u_0 is the rms velocity.

4. Initial conditions and flame parameters

The reacting flow field in a steady opposed jet diffusion flame configuration including a full 40 step chemical kinetic mechanism was obtained using the Sandia code OPPDIF. Pure methane and air at 1 atmosphere, 300°K with a strain rate of approximately 20 $\sec^{-1}$ are the conditions imposed at the fuel and oxidizer jet separated by a distance of 1 cm. These correspond to low strain rate conditions. The strained laminar flame solution from OPPDIF was then allowed to relax to an unstrained condition in the DNS code. The unstrained laminar flame profile was used to initialize all of the species mass fractions, temperature, and density fields in the turbulence simulations.

The DNS was initialized in a two-dimensional computational domain with a plane laminar diffusion flame in the center of the domain. The fuel stream is on the left half of the domain while the oxidizer stream is on the right half of the domain. The velocity field was initialized with the turbulent kinetic energy spectrum given in (20). The turbulence Reynolds number was taken to be 57 based on the turbulence microscale. The flame is thicker than the turbulence microscale but smaller than the turbulence integral scale. Two-dimensional simulations were performed on a 129 by 129 grid.

5. Results and discussion

5.1 Laminar flamelet results

To initialize the direct simulations, the structure for laminar counterflow flamelets were calculated for low strain rates (< 100 $\sec^{-1}$). The details for such calculations may be found in Smooke (1991). Shown in Figs. 1 and 2 are the flamelet structure in mixture fraction space for a global one-step reaction and a three-step mechanism, respectively.

A distinctive qualitative difference between the one-step and three-step mechanism is the broadness of the reaction zone. In Fig. 1c, it can be seen that the consumption of the fuel extends over a much wider range of mixture fraction for the one-step mechanism. The thinness of the fuel-consumption layer in multi-step mechanisms is one of the primary causes of resolution difficulties in direct simulations of turbulent combustion flames. In addition, it can readily be seen in Figs. 1b and 2b that the fuel and oxygen profiles are quite different. In the one-step approximation, fuel leaks through the reaction zone. However, for the three-step mechanism, only oxygen leaks through the reaction layer, which is in agreement with experiments and numerical calculations employing full detailed mechanisms.

Preliminary calculations using the four-step mechanism indicate that the qualitative features of the flamelet agree with previous studies. The major expected difference between the three- and four-step mechanisms is the H atom profile. In the three-step mechanism, all the H is produced on the fuel-lean side of the flamelet and is consumed entirely in the fuel-consumption layer. For the four-step approximation, the H atom profile is broader, in which the fuel-consumption layer is within the H nonequilibrium layer. The monograph by Smooke (1991) may be consulted for

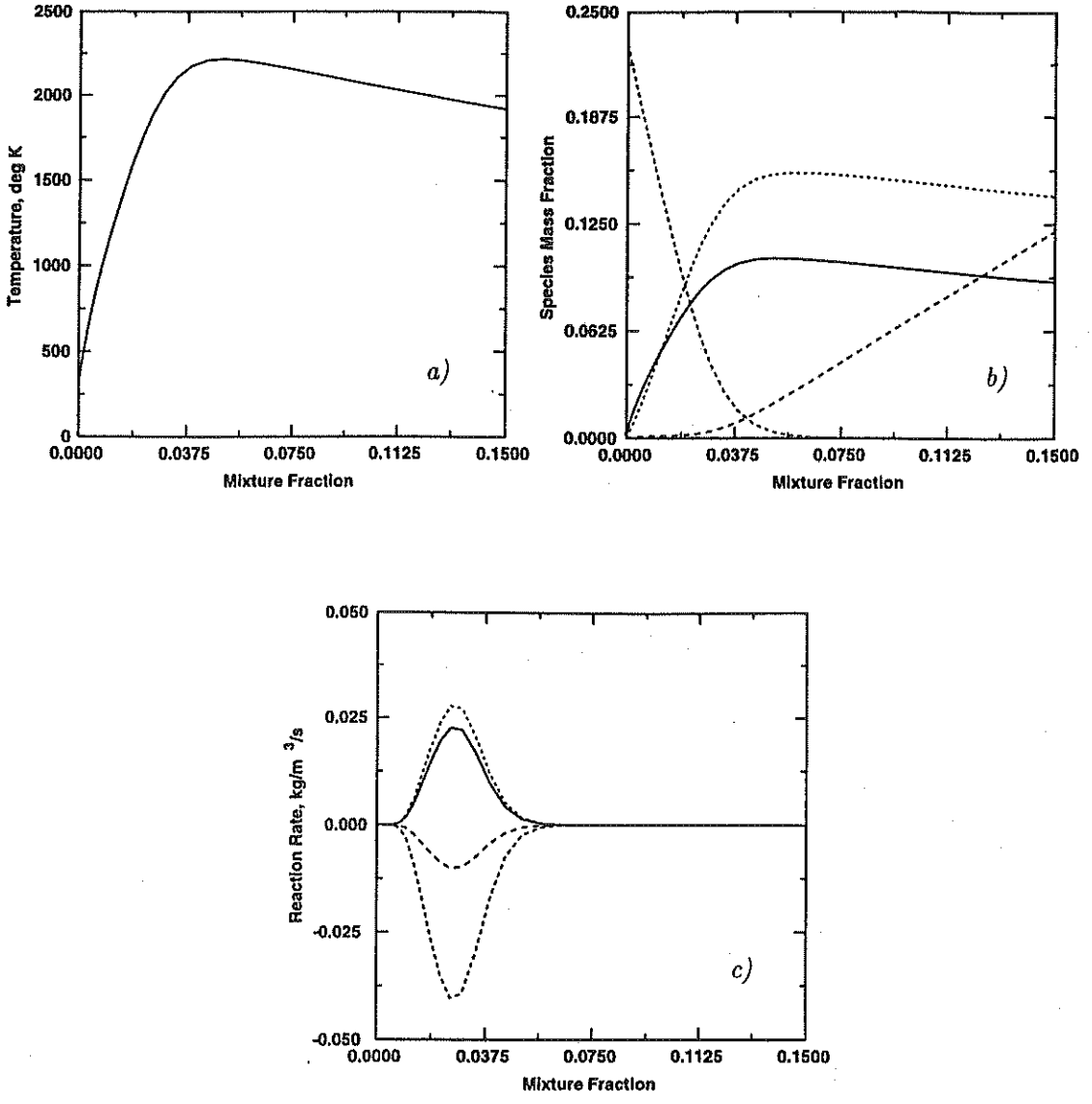

FIGURE 1. One-dimensional unstrained laminar flame for methane-air one-step mechanism: a) temperature, b) species mass fractions, c) species reaction rates. (—— H_2O, ····· CO_2, ····· O_2, ---- CH_4).

more detailed discussion on the structure of laminar methane flames using reduced chemistries.

5.2 Turbulent flame structure

Preliminary results are presented here for the DNS using the global one-step mechanism described in section 2. Simulations are currently underway for the three- and four-step mechanisms. In order to resolve the fuel consumption layer the resolution

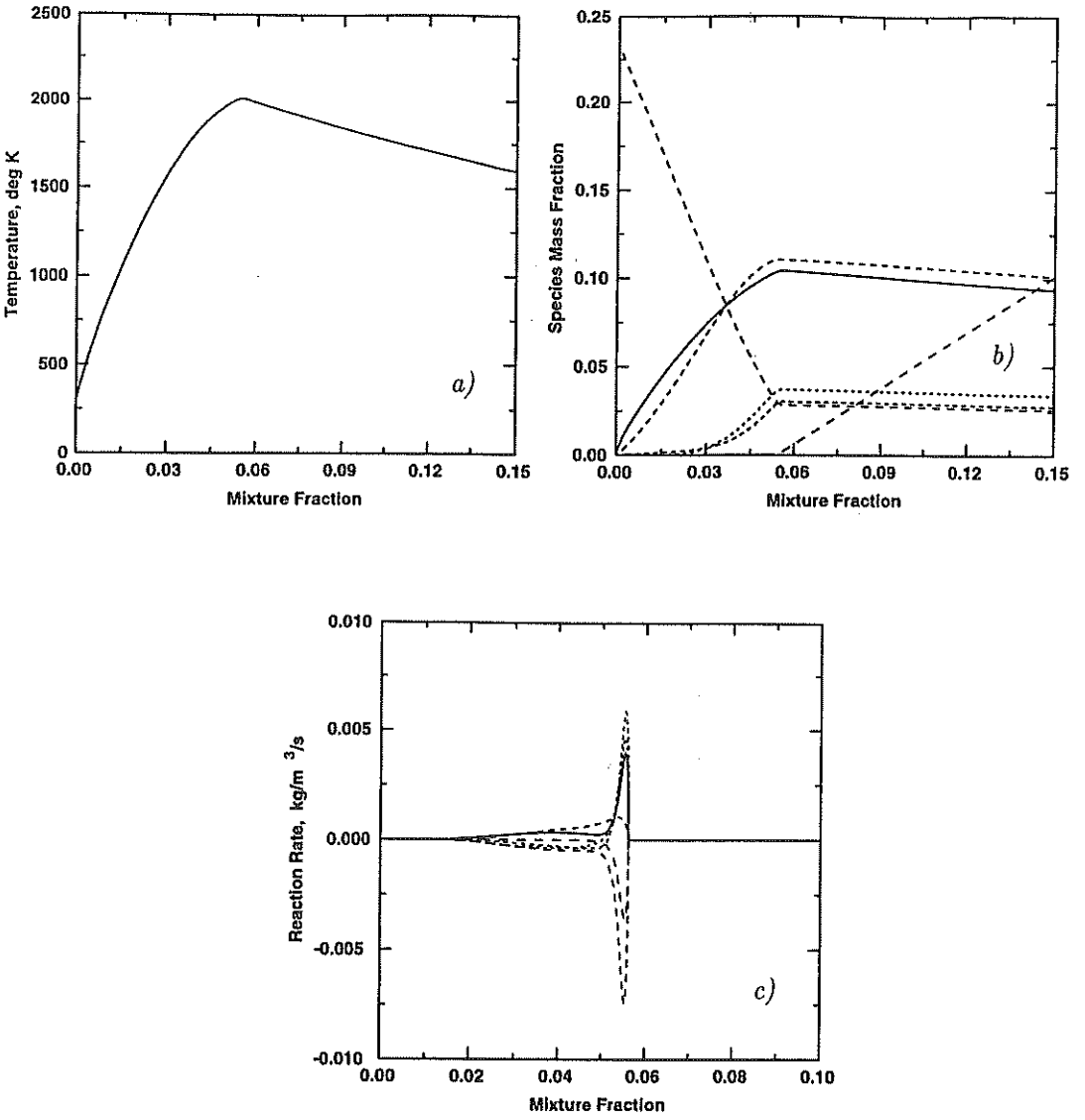

FIGURE 2. One-dimensional strained laminar flame for methane-air three-step mechanism: a) temperature, b) species mass fractions, c) species reaction rates. (—— H_2O, ····· $H_2 * 40$, ····· CO, ---- CO_2, ---- O_2, ---- CH_4).

requirements are much greater for the three- and four-step mechanisms than for the one-step mechanism.

The turbulent two-dimensional DNS was postprocessed at 1.0 and 1.5 turbulent eddy turn times. This is sufficient time for the initial adjustment to occur between the imposed turbulence spectrum and the laminar flame. Instantaneous images of the vorticity magnitude, temperature, reaction rate, and species concentrations at $t = 1.0$ eddy turn time are shown in Fig. 3. It is evident from Fig. 3a that the

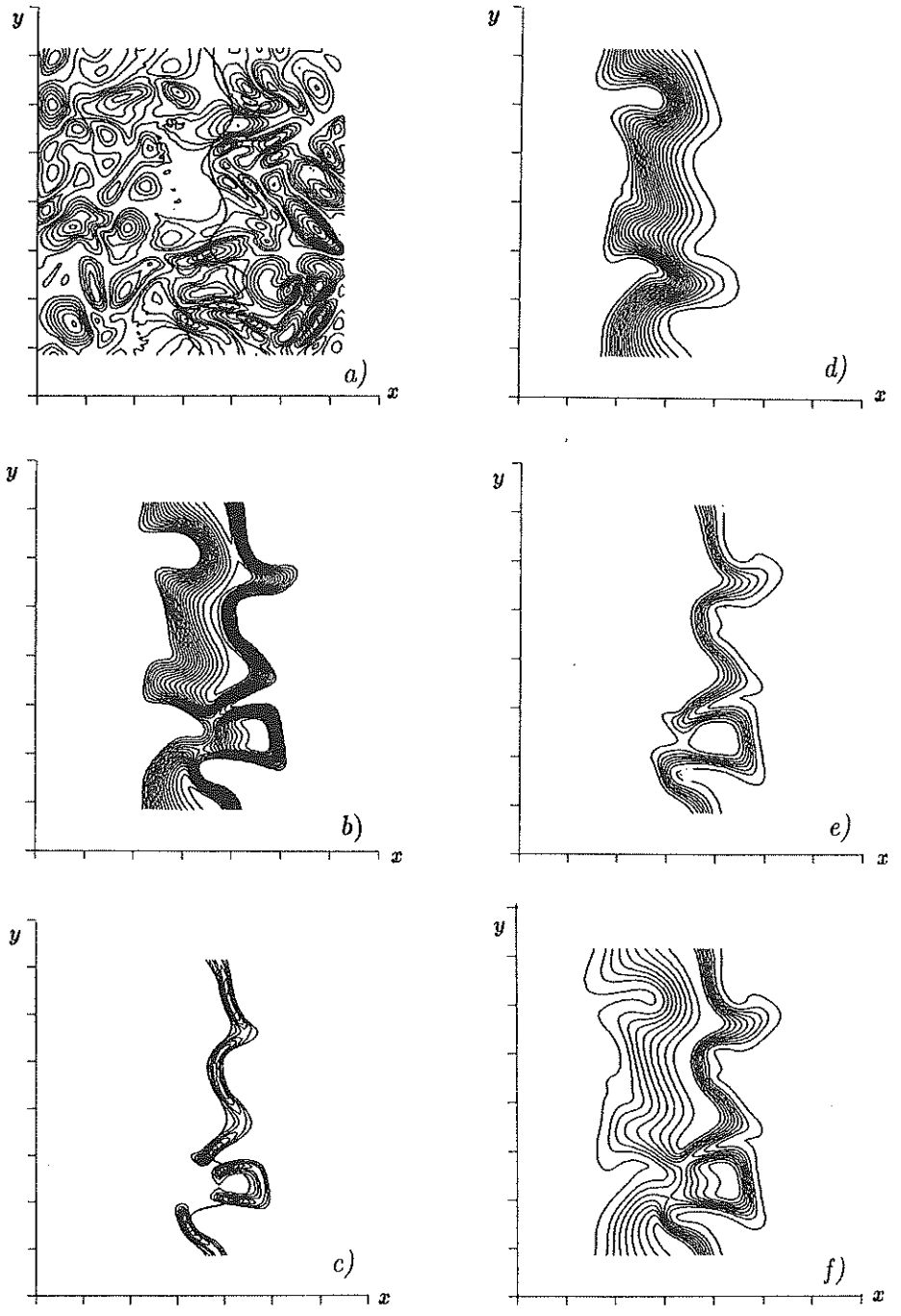

FIGURE 3. Computed fields at 1.0 eddy turn time for the one-step mechanism: a) vorticity magnitude contours with stoichiometric mixture fraction, $f = 0.057$, b) temperature, c) CH_4 reaction rate with $f = 0.057$, d) CH_4 mass fraction, e) O_2 mass fraction, f) CO_2 mass fraction.

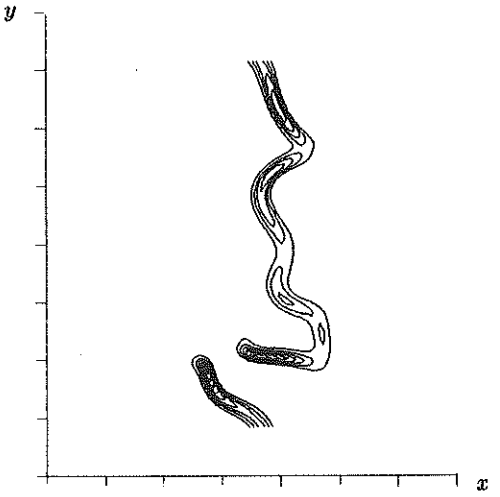

FIGURE 4. CH_4 reaction rate at 1.5 eddy turn times.

vorticity is greatly dampened in the vicinity of the reaction zone. The turbulence was initialized at all locations in the computational domain except near the outflow boundaries normal to the flame. Due to a combination of dilatational effects and a substantial increase in the kinematic viscosity with temperature, vorticity in the vicinity of the flame is dampened. Note in Fig. 3c that the vorticity is dampened more on the fuel side than on the oxidizer side. This is due to the lower density (higher temperature) that exists on the rich side of the flame which results in a higher kinematic viscosity on that side.

While the effect of the heat release is to weaken the turbulence, the effect of the turbulence is to wrinkle the flame. There are regions where the flame is locally extinguished as shown by the discontinuities in the reaction rate contour lines shown in Fig. 3c. At a later time in the simulation, $t = 1.5$ eddy turn times, the conditions are such that locally the strain rate is reduced in regions with hot products due to the heat release. The hot products act as an ignition source and in locations where fuel and oxidizer are present, the flame starts to burn once again. A comparison of Fig. 4 and Fig. 3c shows a region where reignition occurs. Previous simulations with simple chemistry (Chen 1992a, 1992b) did not report the occurrence of reignition.

It is also observed from the reaction rate contours and the stoichiometric mixture fraction line (Fig. 3c) that the flame does not always burn at the stoichiometric mixture fraction. Near the peak reaction rates the flame is stoichiometric; however, in regions that are curved toward the oxidizer stream the flame tends to burn lean, whereas in regions that are curved toward the fuel stream the flame tends to burn rich. We suspect that this is a Lewis number effect and that it is particularly pronounced in regions having the largest curvature. In regions that are curved toward

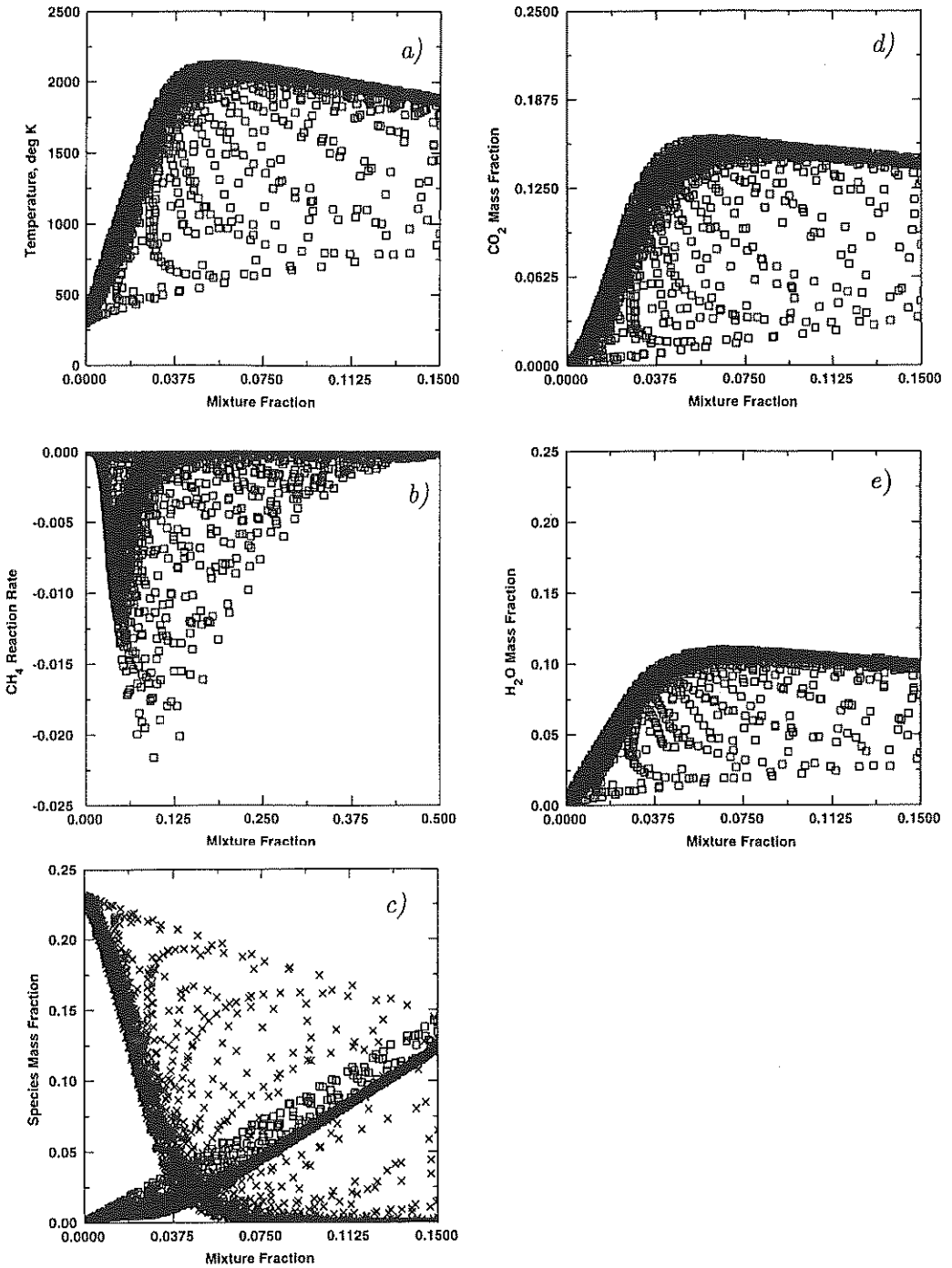

FIGURE 5. Scatter plots at 1.0 eddy turn time for one-step mechanism: a) temperature, b) CH_4 reaction rate, c) CH_4 and O_2 mass fraction (□ CH_4, × O_2), d) CO_2 mass fraction, and e) H_2O mass fraction.

the oxidizer, the defocusing of methane overcomes the greater mass diffusivity of methane ($Le = 0.97$) over oxygen ($Le = 1.11$). Hence, the flame tends to burn lean. On the other hand, in regions that are curved towards the fuel, the additive effect of focusing the methane combined with its larger mass diffusivity leads to a situation where there is an abundance of methane at the reaction zone. Hence, in this situation the flame tends to burn rich, and eventually, as the curvature becomes too large, the flame becomes too rich to burn, at which point local extinction occurs first at the flame tip. Since the reactant Lewis numbers in the DNS can readily be interchanged, these influences will be studied in greater detail in future simulations.

The reactant and product concentrations are presented in Figs. 3d-3f. Note that CH_4 is more diffusive than O_2. The products CO_2 and H_2O follow the temperature (Fig. 3b) quite closely; hence, for the sake of brevity, only CO_2 is presented in Fig. 3f.

Scatter plots of the temperature, CH_4 reaction rate, and species concentrations in mixture fraction space are shown in Fig. 5. The mixture fraction, f, is defined to be zero in the oxidizer stream and unity in the fuel stream. The maximum temperature occurs near the stoichiometric mixture fraction, $f = 0.057$. The CH_4 reaction rate peak is shifted slightly toward the fuel side. Consistent with the physical representation of the flame, the presence of both high and low values of the temperature and reaction rate in Figs. 5a and 5b suggests that there are regions in the flame that are fully burning as well as other regions that are being extinguished by the local strain-rate field. From Fig. 5c, note that there is leakage of both CH_4 and O_2 in this one-step model. Also, a significant portion of the flame is undergoing various stages of extinction as indicated by the spread of points between the equilibrium and frozen flow limits.

6. Concluding remarks

Preliminary results from DNS demonstrate that two-dimensional simulations of turbulent non-premixed methane-air flames modeled with reduced chemistry are feasible. The global one-step simulation required 50 cpu hours on a Cray-YMP. Extensions to three- and four-step mechanisms requires resolving the fuel consumption layer of the flame, a region that is approximately an order of magnitude smaller than the overall flame thickness. Simulations on a uniform grid will have enormous resolution requirements if the internal flame structure is to be fully resolved. This suggests a real need for a local adaptive mesh refinement capability for simulations of hydrocarbon flames.

Once the three- and four-step simulations are completed, detailed comparisons of the internal flame structure and extinction characteristics will be made. In particular, strain-rate and curvature statistics will be obtained and comparisons of the turbulence simulations with steady one-dimensional strained laminar flame predictions will be made. Finally, reduced mechanisms for the formation of thermal and prompt NO_x will be evaluated from the major species concentrations and the temperature.

Acknowledgements

This research was supported by the Center for Turbulence Research and the

Department of Energy, Division of Basic Energy Sciences. One of us (SM) acknowledges partial funding through the AWU-DOE faculty fellowship program. The authors are grateful to their CTR hosts T. Mantel, G. Reutsch, and J. M. Samaniego for their excellent arrangements. We would also like to thank A. Liñán, T. Poinsot, A. Trouvé, and T. Echekki for many insightful discussions.

REFERENCES

BAUM, M., POINSOT, T., & HAWORTH, D. 1992 Numerical simulations of turbulent premixed $H_2/O_2/N_2$ flames with chemistry. *Proceedings of the 1992 Summer Program.* Center for Turbulence Research, NASA Ames/Stanford Univ., 345-366.

CHEN, J., MAHALINGAM, S., PURI, I., & VERVISCH, L. 1992a Effect of finite-rate chemistry and unequal Schmidt numbers on turbulent non-premixed flames modeled with single-step chemistry. *Proceedings of the 1992 Summer Program.* Center for Turbulence Research, NASA Ames/Stanford Univ., 367-387.

CHEN, J., MAHALINGAM. S., PURI, I., & VERVISCH, L. 1992b Non-premixed flames modeled with two-step chemistry. *Proceedings of the 1992 Summer Program.* Center for Turbulence Research, NASA Ames/Stanford Univ., 389-402.

BUI-PHAM, M. N. 1992 Studies in structures of laminar hydrocarbon flames. Ph.D. Dissertation, University of California, San Diego.

KEE, R. J., RUPLEY, F. M., & MILLER, J. A. 1987 The Chemkin Thermodynamic Database. *SAND-8215B.*

LELE, S. 1992 Compact finite difference schemes with spectral-like resolution. *J. Comput. Phys.*, (to appear).

MAHALINGAM, S., CHEN, J., & VERVISCH, L. 1994 Finite-rate chemistry and transient effects in direct numerical simulations of turbulent non-premixed flames. *Comb. & Flame* (submitted).

MONTGOMERY, C. J., KOSALY, G. & RILEY, J. J. 1992 Direct numerical simulations of turbulent H_2-O_2 combustion using reduced chemistry. Submitted for presentation at the 31st AIAA Aerospace Sciences Meeting to be held at Reno, NV, January, 1993.

PETERS, N. 1985 Numerical and Asymptotic Analysis of Systematically Reduced Reaction Schemes for Hydrocarbon Flames. *Numerical Simulation of Combustion Phenomena.* Lecture Notes in Physics, **241,** 90-109.

PETERS, N. 1986 Laminar flamelet concepts in turbulent combustion. *Twenty-First Symposium (International) on Combustion.* The Combustion Institute. 1231-1250.

PETERS, N. & ROGG, B. (ED.) 1993 Reduced kinetic mechanisms for applications in combustion systems. *Lecture Notes in Physics m15,* Springer-Verlag, New York.

PETERS, N. & WILLIAMS, F. A. 1987 The asymptotic structure of stoichiometric methane-air flames. *Comb. & Flame.* **68,** 185.

POINSOT, T., AND LELE, S. 1991 Boundary conditions for direct simulations of compressible viscous flows. *J. Comput. Phys.* **101,** No 1.

PURI, I. K., SESHADRI, K., SMOOKE, M. D. AND KEYES, D. E. 1987 A comparison between numerical calculations and experimental measurements of the structure of a counterflow methane-air diffusion flame. *Comb. Science and Tech.* **56,** 1.

SESHADRI, K. AND PETERS, N. 1988 Asymptotic structure and extinction of methane-air diffusion flames. *Comb. & Flame.* **73,** 23.

SMOOKE, M. D. (ED.) 1991 in Reduced kinetic mechanisms and asymptotic approximation for methane-air flames. *Lecture Notes in Physics 384,* Springer-Verlag, New York.

WILLIAMS, F. A. 1985 Combustion theory, second edition. Addison/Welsly.